Annual Report Vol. 43 (2020)

Quantifying rates of Quaternary landscape evolution in Grand Teton National Park using in situ cosmogenic ^{10}Be, ^{14}C, and ^{36}Cl dating

Alia Lesnek[1,2*] and Joseph Licciardi[1]

1 Department of Earth Sciences, University of New Hampshire, Durham, NH
2 School of Earth and Environmental Sciences, Queens College, CUNY, Queens, NY
* Author for correspondence: alia.lesnek@qc.cuny.edu

Abstract In Grand Teton National Park (GTNP), both glacial and tectonic activity have played major roles in shaping the landscape. Here, we evaluate the impacts of late Quaternary Teton Fault slip and subglacial erosion in GTNP. We are in the process of using ^{10}Be surface exposure dating to generate records of time-integrated Teton Fault slip at multiple locations throughout GTNP, which will allow us to assess spatial and temporal patterns of tectonic activity over the past ~15 ka. We are also working to determine rates of subglacial erosion through ^{10}Be-^{14}C-^{36}Cl triple isotope dating. The results obtained through this novel combination of cosmogenic nuclide techniques will contribute toward a unified view of landscape evolution in alpine environments.

Introduction

Glacial erosion and tectonism are powerful agents of landscape change, and together are responsible for creating some of the most dramatic topographic relief on Earth (Thomson et al., 2010). Understanding the past, present, and future evolution of Earth's surface requires quantitative assessments of climatically- and tectonically-driven disturbances (NASEM, 2020). The iconic landscapes of Grand Teton National Park (GTNP) provide an ideal natural laboratory for such investigations. Here, we evaluate the impacts of late Quaternary glaciation and tectonism on landscape evolution in GTNP. To achieve this goal, we will develop quantitative records of time-integrated Teton fault slip and subglacial erosion through cosmogenic nuclide dating methods. Our specific aims include (1) generating ^{10}Be surface exposure chronologies of fault-offset depositional features, which will allow us to constrain offset rates; and (2) triple-isotope cosmogenic surface exposure dating of bedrock in valleys along the eastern Teton Range to reconstruct glacial history and subglacial erosion rates.

Background

Teton Fault motion

Much of the topographic relief in the Teton Range can be attributed to uplift along the Teton fault, an eastward-dipping, range-bounding normal fault that extends ~70 km along the eastern front of the range (Figure 1; Smith et al., 1993). Total stratigraphic offset along the Teton fault far exceeds present topographic relief (~2 km) and is estimated to be 6-9 km since its inception between 13 and 5 Ma (Smith et al., 1993). Well-preserved fault scarps displacing Pinedale-age glacial moraines (Licciardi and Pierce, 2008; Pierce et al., 2018) and disturbed sediment layers in fault trenches (Byrd et al., 1994; Zellman et al., 2020) provide convincing evidence for late Pleistocene and Holocene fault activity. Estimates of Pleistocene-Holocene Teton fault slip range from 1.0

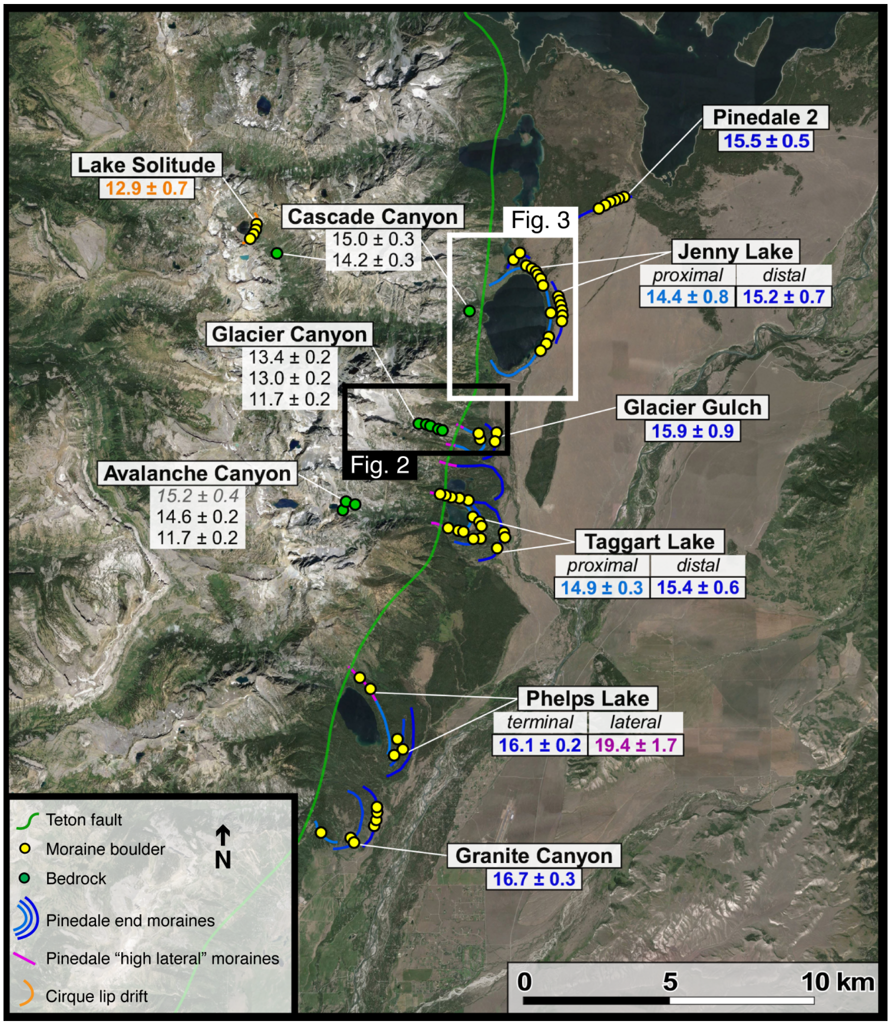

Figure 1. Map of GTNP with ^{10}Be ages of end moraines, lateral moraines, and glacially-scoured bedrock. ^{10}Be ages shown in ka at 1 standard deviation internal uncertainty. Modified from Pierce et al. (2018)

and 5.0 mm a^{-1} (Pierce and Haller, 2011), but recent work suggests that slip rates may have been both temporally-and spatially-variable (e.g., Thackray and Staley, 2017; DuRoss et al., 2020; Hampel et al., 2021). A paleoseismic record from Jenny Lake sediments confirms these inferences, indicating that large-magnitude seismic events occurred more frequently immediately following regional deglaciation at ∼15 ka (Larsen et al., 2019). However, these records come from a select few locations within GTNP (Figure 1) and provide integrated fault offset information for only three time intervals: 15-10 ka, 10-8 ka, and 8-5 ka. To fully assess the spatial and temporal variations in Teton fault motion, there is a need for additional, quantitative fault offset reconstructions from other locations and landforms within GTNP.

Subglacial erosion

During the Pinedale glaciation, which culminated at ∼15 ka in the eastern Teton Range, alpine glaciers extended into Jackson Hole, building suites of large, well-preserved moraines (Figure 1; Licciardi and Pierce, 2008; Pierce et al., 2018). Recession from the Pinedale end moraines progressed quickly, reaching the cirque at Lake Solitude by ∼13 ka (Licciardi and Pierce, 2008). Similarly, bedrock ^{10}Be ages from Glacier and Avalanche Canyons suggest rapid glacial retreat from the Pinedale maximum positions (Figure 1). Although the chronology of glacial activity in the eastern Teton Range is relatively well-constrained, few quantitative estimates of subglacial erosion rates exist for GTNP. Estimates of basin-averaged erosion rates are on the order of 0.2 mm a^{-1} since the Pinedale glaciation (Tranel et al., 2015) and likely varied on glacial-interglacial timescales (Tranel et al., 2011). However, these studies did not quantify the subglacial component of erosion, but rather integrated the effects of multiple processes acting on the landscape.

Recent research suggests that the efficiency of subglacial erosion is related to sliding velocity, and that the highest sliding velocities are achieved in settings with high mean annual precipitation (Cook et al., 2020). The Teton Range has a dramatic gradient in modern mean annual precipitation, with a nearly order of magnitude difference in precipitation amounts between its eastern and western flanks (Daly et al., 2008). During the Pinedale glaciation, this contrast may have been even more pronounced (Foster et al., 2010). Ongoing work in the western Teton Range indicates that those glaciers experienced at least one readvance after regional deglaciation, and that these readvance phases were minimally-erosive (Ward et al., 2019). This scenario may have also occurred in the eastern Teton Range. Three ^{10}Be ages from bedrock in Glacier Gulch do not get progressively younger upvalley (Figure 2), which would be expected under a scenario of monotonic ice retreat with high rates of subglacial erosion.

Research questions

The overall goal of this project is to generate new quantitative estimates of landscape change that can be used to assess the relative roles of glaciation and tectonism in driving Quaternary landscape evolution in GTNP. We have undertaken a targeted campaign of cosmogenic nuclide dating in the eastern Teton Range to address the following research questions:

What are the spatial and temporal patterns of Teton fault motion during the Late Pleistocene and Holocene? We targeted large, stable boulders on the surfaces of fault-offset depositional features for ^{10}Be surface exposure dating (Figures 3 and 4). By combining the ^{10}Be ages with published estimates of fault offset and/or slip from LiDAR (Thackray and Staley, 2017; Hampel et al., 2021), we will be able to generate centennial-scale reconstructions of cumulative fault motion at multiple locations.

What is the late Pleistocene glacial and glacio-erosional history of valleys draining the eastern Teton Range? We will reconstruct the history of deglaciation and glacial erosion from triple-isotope cosmogenic nuclide dating in Glacier Gulch (Figure 2). We will measure the concentrations of three cosmogenic isotopes in bedrock surfaces: ^{10}Be, in situ ^{14}C, and ^{36}Cl. The concentrations of these isotopes in bedrock surfaces reflect the interplay between ice/snow cover, glacial erosion, and exposure.

Methods

To address our research questions and quantify rates of Quaternary landscape evolution in Grand Teton National Park, we measure concentrations of in situ cosmogenic nuclides in exposed rock surfaces. Over the past few decades, in situ cosmogenic nuclides have emerged as the “standard method” for dating both glacial and fluvial landforms (Granger et al., 2013). These techniques rely on the production of rare isotopes within mineral crystal lattices when rock surfaces are exposed to cosmic radiation (Gosse and Phillips, 2001). The accumulation of these cosmogenic isotopes occurs in the upper ∼2-3 m of rock surfaces and is directly related to the duration of surface exposure. Thus, by measuring the concentration of a particular cosmogenic nuclide and dividing that value by a site-specific production rate (e.g., Lifton et al., 2014, 2015), we are able to calculate an exposure age for a given rock surface.

Quantifying fault offset rates using ^{10}Be surface exposure dating

The age of Quaternary depositional features such as alluvial fans and debris flows will be developed using ^{10}Be surface exposure dating techniques. Exposure ages for boulders on the uppermost surface should correspond to the final stage of fan construction. If a feature is offset by a preserved fault scarp, the

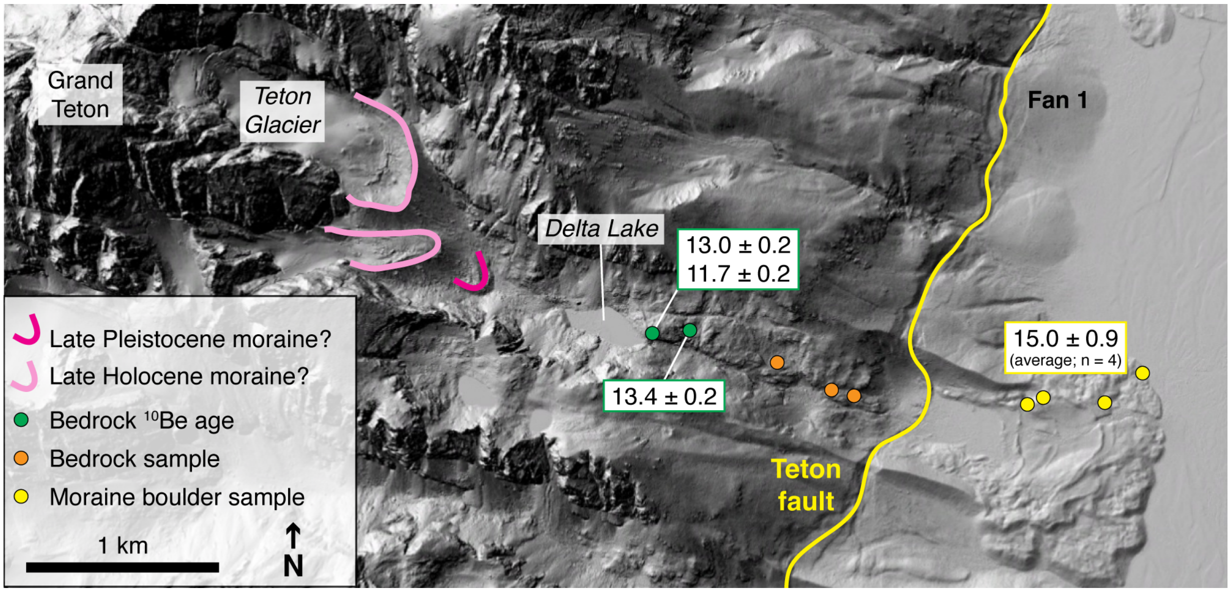

Figure 2. Map of Glacier Gulch. Average ^{10}Be ages from moraine boulders (yellow dots; Pierce et al., 2018) and individual ^{10}Be ages from bedrock (green dots; Pierce et al., 2018) are indicated at 1 standard deviation internal uncertainty. Locations of new bedrock samples that are in processing are shown as orange dots.

modern displacement must have accumulated after the surface was abandoned. Measurements of feature age and fault offset can therefore be used to determine cumulative offset rates since the feature was constructed (e.g., Ritz et al., 1995; Siame et al., 1997; Frankel et al., 2007).

Quantifying subglacial erosion rates using triple-isotope dating

In simple cases, ^{10}Be surface exposure dating of bedrock will provide the timing of glacial retreat (Balco, 2011). However, in environments where erosion is insufficient to remove the upper 2-3 meters of rock, "inherited" cosmogenic isotopes from prior exposure periods remain within a rock surface. While this issue can complicate interpretations of glacial history when using a single cosmogenic isotope, measuring the concentrations of multiple cosmogenic isotopes can provide insight into complex glacial history and glacial erosion. We will measure in situ ^{14}C, ^{10}Be, and ^{36}Cl in bedrock surfaces in Glacier Gulch because the ratios between these cosmogenic isotope concentrations reflect both the amount of subglacial erosion and the timing of deglaciation (Ward et al., 2019).

Preliminary results

Fault offset rates

In fall 2019, we collected five rock samples for ^{10}Be dating from an alluvial fan just south of Jenny Lake (Fan 1; Figure 3). The fan has a LiDAR-derived vertical separation of 13.9 ± 1.1 m (Thackray and Staley, 2017). This fan had never been directly dated. However, Thackray and Staley (2017) estimated its age as 29.1 ± 7.0 ka by assuming a constant slip rate of 0.82 ± 0.13 mm a^{-1} since fan deposition. Our samples included four large boulders from the fan surface and one water-scoured bedrock sample from an abandoned channel above the fan (Figure 2). These samples are being prepared for analysis at the University of New Hampshire.

In summer 2021, we collected ten rock samples from two debris flows near String Lake for ^{10}Be dating (Figure 3). One of these features (the 'String Lake' debris flow) is offset by the Teton Fault. Recent work suggests the magnitude of vertical fault slip on the String Lake debris flow is 25.3 ± 2.5 m (Hampel et al., 2021). Similar to our approach at Fan 1, ^{10}Be ages from the String Lake debris flow will constrain the time

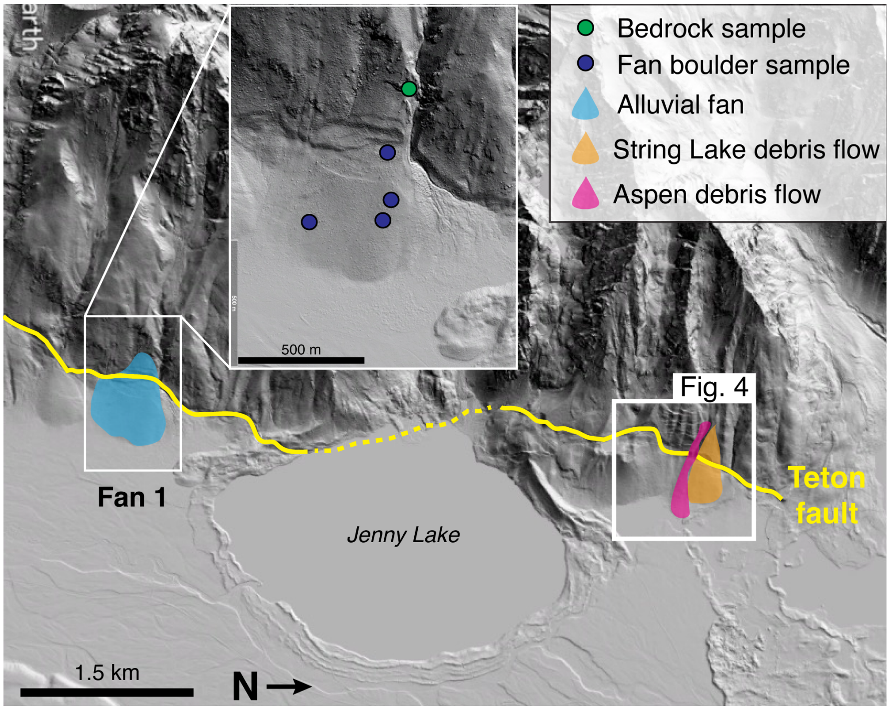

Figure 3. LiDAR DEM showing the locations of Fan 1 (blue shading) and the two debris flows near String Lake (pink and orange shading). Boulder (dark blue) and bedrock (green) samples collected from Fan 1 are shown by colored dots.

that has elapsed since the debris flow occurred. By combining the new ^{10}Be ages with the Hampel et al. (2021) estimate of vertical Teton Fault slip at this location, we will be able to determine time-integrated Teton Fault slip rate. In contrast, the second debris flow (the 'Aspen' debris flow) does not appear to be offset by the Teton Fault (Figure 4). Thus, ages from the surface of the Aspen debris flow should provide a minimum constraint on the timing of the last major rupture of the Teton Fault. Processing for these ten samples is currently underway at the University of New Hampshire, and we expect to have ^{10}Be ages by Spring 2022. Taken together, the debris flows at this site will provide key information about the temporal variations in Teton Fault slip.

Subglacial erosion

At Glacier Gulch, we collected three bedrock samples for triple isotope dating (Figure 2). At the time of this writing, all samples have been processed for ^{10}Be, and preparations for ^{14}C and ^{36}Cl extractions are underway at the University of New Hampshire. Once all isotope concentrations have been obtained, we will use a Monte Carlo-based inversion model (Ward et al., 2019) to evaluate potential exposure, burial, and erosion scenarios. These results are anticipated to provide new insights into the patterns of subglacial erosion in alpine catchments.

Conclusions

Thus far, our work in GTNP suggests that offset along the Teton Fault is both spatially and temporally variable. Records of past fault motion may help to improve geologic hazard assessments on both local and regional scales. Although we do not yet have new triple isotope data from Glacier Gulch, we hope that the results will allow for a more comprehensive assessment of patterns of glacier erosion in alpine environments and, more specifically, contribute towards a better understanding of Pleistocene glacier change in the Tetons. When complete, this project will provide new constraints on Quaternary landscape evolution in GTNP and alpine settings in general.

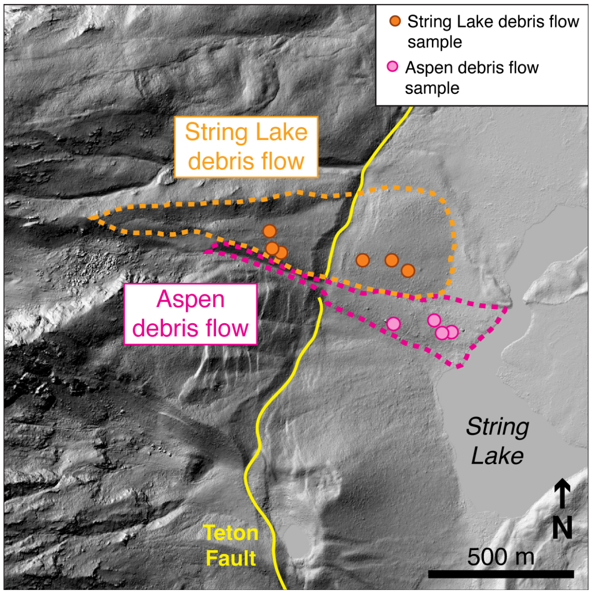

Figure 4. LiDAR DEM showing the locations of debris flows in north-central GTNP. Teton Fault trace indicated by the yellow line. Outlines of slope failure scarps and runouts shown by the dotted lines. Colored dots indicate locations of samples collected for ^{10}Be dating in summer 2021.

Future work

Future work on this project will include final processing of our cosmogenic isotope samples. We anticipate that final results will be available in spring 2022. By better reconstructing glacial history, we will gain an increased understanding of biotic response to past climate change, as well as essential context for paleoecological studies (e.g., Whitlock, 1993; Krause et al., 2015). Ultimately, integrating our results with model simulations of past Teton fault motion (e.g., Hampel et al., 2007) would be useful to evaluate the effects of climate-related processes such as glacial isostatic rebound on tectonic activity and landscape evolution.

Acknowledgements

Major funding for this research was provided by the UW-NPS small grants program. We thank Glenn Thackray for discussions about Teton Fault slip measurements. We would also like to thank Darren Larsen, Avriel Licciardi, Naomi Ochwat, and Michael Waterman for field support.

References

Balco, G. 2011. Contributions and unrealized potential contributions of cosmogenic-nuclide exposure dating to glacier chronology, 1990–2010. Quaternary Science Reviews **30**:3–27. http://www.sciencedirect.com/science/article/pii/S0277379110003999.

Byrd, J. O. D., R. B. Smith, and J. W. Geissman. 1994. The Teton fault, Wyoming: Topographic signature, neotectonics, and mechanisms of deformation. Journal of Geophysical Research: Solid Earth **99**:20095–20122.

Cook, S. J., D. A. Swift, M. P. Kirkbride, P. G. Knight, and R. I. Waller. 2020. The empirical basis for modelling glacial erosion rates. Nature communications **11**:759. https://doi.org/10.1038/s41467-020-14583-8.

Daly, C., M. Halbleib, J. I. Smith, W. P. Gibson, M. K. Doggett, G. H. Taylor, J. Curtis, and P. P. Pasteris. 2008. Physiographically sensitive mapping of climatological temperature and precipitation across the conterminous United States. International Journal of Climatology: A Journal of the Royal Meteorological Society **28**:2031–2064.

DuRoss, C. B., R. D. Gold, R. W. Briggs, J. E. Delano, D. A. Ostenaa, M. S. Zellman, N. Cholewinski, S. J. Wittke, and S. A. Mahan. 2020. Holocene earthquake history and slip rate of the southern Teton fault, Wyoming, USA. Bulletin **132**:1566–1586.

Foster, D., S. H. Brocklehurst, and R. L. Gawthorpe. 2010. Glacial-topographic interactions in the Teton Range, Wyoming. Journal of Geophysical Research: Earth Surface **115**.

Frankel, K. L., J. F. Dolan, R. C. Finkel, L. A. Owen, and J. S. Hoeft. 2007. Spatial variations in slip rate along the Death Valley-Fish Lake Valley fault system determined from LiDAR topographic data and cosmogenic ^{10}Be geochronology. Geophysical Research Letters **34**.

Gosse, J. C., and F. M. Phillips. 2001. Terrestrial in situ cosmogenic nuclides: Theory and application. Quaternary Science Reviews **20**:1475–1560. http://dx.doi.org/10.1016/S0277-3791(00)00171-2http://www.sciencedirect.com/science/article/pii/S0277379100001712.

Granger, D. E., N. A. Lifton, and J. K. Willenbring. 2013. A cosmic trip: 25 years of cosmogenic nuclides in geology. Geological Society of America Bulletin **125**:1379–1402.

Hampel, A., R. Hetzel, and A. L. Densmore. 2007. Postglacial slip-rate increase on the Teton normal fault, northern Basin and Range Province, caused by melting of the Yellowstone ice cap and deglaciation of the Teton Range? Geology **35**:1107–1110.

Hampel, A., R. Hetzel, and M.-S. Erdmann. 2021. Postglacial slip distribution along the Teton normal fault (Wyoming, USA), derived from tectonically offset geomorphological features. Geosphere **17**:1517–1533. https://doi.org/10.1130/GES02370.1.

Krause, T. R., Y. Lu, C. Whitlock, S. C. Fritz, and K. L. Pierce. 2015. Patterns of terrestrial and limnologic development in the northern Greater Yellowstone Ecosystem (USA) during the late-glacial/early-Holocene transition. Palaeogeography, Palaeoclimatology, Palaeoecology **422**:46–56.

Larsen, D. J., S. E. Crump, M. B. Abbott, W. Harbert, A. Blumm, N. J. Wattrus, and J. J. Hebberger. 2019. Paleoseismic evidence for climatic and magmatic controls on the Teton fault, WY. Geophysical Research Letters **46**:13036–13043.

Licciardi, J. M., and K. L. Pierce. 2008. Cosmogenic exposure-age chronologies of Pinedale and Bull Lake glaciations in greater Yellowstone and the Teton Range, USA. Quaternary Science Reviews **27**:814–831.

Lifton, N., M. Caffee, R. Finkel, S. Marrero, K. Nishiizumi, F. M. Phillips, B. Goehring, J. Gosse, J. Stone, J. Schaefer, B. Theriault, A. J. T. Jull, and K. Fifield. 2015. In situ cosmogenic nuclide production rate calibration for the CRONUS-Earth project from Lake Bonneville, Utah, shoreline features. Quaternary Geochronology **26**:56–69. http://www.sciencedirect.com/science/article/pii/S1871101414001101.

Lifton, N., T. Sato, and T. J. Dunai. 2014. Scaling in situ cosmogenic nuclide production rates using analytical approximations to atmospheric cosmic-ray fluxes. Earth and Planetary Science Letters **386**:149–160. http://www.sciencedirect.com/science/article/pii/S0012821X13006316.

National Academies of Sciences, Engineering, and Medicine (NASEM). 2020. A vision for NSF Earth sciences 2020-2030: Earth in time. National Academies Press.

Pierce, K. L., and K. M. Haller, 2011. Teton fault, central section. https://earthquakes.usgs.gov/hazards/qfaults.

Pierce, K. L., J. M. Licciardi, J. M. Good, and C. Jaworowski. 2018. Pleistocene glaciation of the Jackson Hole area, Wyoming.

Ritz, J. F., E. T. Brown, D. L. Bourles, H. Philip, A. Schlupp, G. M. Raisbeck, F. Yiou, and B. Enkhtuvshin. 1995. Slip rates along active faults estimated with cosmic-ray–exposure dates: Application to the Bogd Fault, Gobi-Altaï, Mongolia. Geology **23**:1019–1022.

Siame, L. L., D. L. Bourlès, M. Sébrier, O. Bellier, J. C. Castano, M. Araujo, M. Perez, G. M. Raisbeck, and F. Yiou. 1997. Cosmogenic dating ranging from 20 to 700 ka of a series of alluvial fan surfaces affected by the El Tigre fault, Argentina. Geology **25**:975–978.

Smith, R. B., J. O. D. Byrd, and D. D. Susong. 1993. The Teton fault, Wyoming: Seismotectonics, Quaternary history, and earthquake hazards. Geology of Wyoming: Geological Survey of Wyoming Memoir **5**:628–667.

Thackray, G. D., and A. E. Staley. 2017. Systematic variation of Late Pleistocene fault scarp height in the Teton Range, Wyoming, USA: Variable fault slip rates or variable landform ages? Geosphere **13**:287–300.

Thomson, S. N., M. T. Brandon, J. H. Tomkin, P. W. Reiners, C. Vásquez, and N. J. Wilson. 2010. Glaciation as a destructive and constructive control on mountain building. Nature **467**:313–317.

Tranel, L. M., J. A. Spotila, S. A. Binnie, and S. P. H. T. Freeman. 2015. Quantifying variable erosion rates to understand the coupling of surface processes in the Teton Range, Wyoming. Geomorphology **228**:409–420.

Tranel, L. M., J. A. Spotila, M. J. Kowalewski, and C. M. Waller. 2011. Spatial variation of erosion in a small, glaciated basin in the Teton Range, Wyoming, based on detrital apatite (U-Th)/He thermochronology. Basin Research **23**:571–590.

Ward, D., J. M. Licciardi, and B. M. Goehring, 2019. Three-isotope cosmogenic dating reveals a complex deglaciation history in the western Teton Range. Pages ep33a–04 . AGU.

Whitlock, C. 1993. Postglacial vegetation and climate of Grand Teton and southern Yellowstone National Parks. Ecological Monographs **63**:173–198.

Zellman, M. S., C. B. DuRoss, G. D. Thackray, S. F. Personius, N. G. Reitman, S. A. Mahan, and C. C. Brossy. 2020. Holocene Rupture History of the Central Teton Fault at Leigh Lake, Grand Teton National Park, Wyoming. Bulletin of the Seismological Society of America **110**:67–82.